Supplementary information for

Jet-cooled vibronic spectroscopy of phenylcyclopentenes: I. S_0 and S_1 torsional potentials in phenylcyclopentadi-1,3-ene

Josh J. Newby, Ching-Ping Liu,† Christian W. Müller, and Timothy S. Zwier*
Department of Chemistry, Purdue University,
West Lafayette, IN 47907-2084 U.S.A.

Contents

Figure S1: Extended, saturated R2PI spectrum showing very weak transitions over 400 cm^{-1} above the electronic origin transition.

Table S1: Assignments for the LIF spectrum of PCP3D.

Table S2: Complete Assignments of the SVLF of PCP3D

Table S3: Calculated torsional angles and torsional vibrational frequencies for the two isomers of PCPD that are expected to be in the probed spectra region.

Figure S2: Calculated torsional potentials for PCP4D in the S_0 (lower) and S_1 (upper) states. The S_0 potential was calculated at the B3LYP//6-311+G(d,p) level of theory while the S_1 was computed using CIS//6-311+G(d,p).

A note on calculating Frank-Condon intensities for hot band spectra

Figure S3: Franck-Condon intensity simulations of the (a) LIF spectrum and (b) SVLF spectrum of the 57^1_1 transitions. The LIF simulation assumes a vibrational temperature of 9.8 K. The resonance fluorescence band was cut off in the 57^1_1 band SVLF spectrum as most of the observed intensity was due to incomplete subtraction of scattered light from the laser.

Figure S4: Calculated molecular orbitals (CIS//6-311+G(d,p)) for PCP3D. Since the calculated $S_1 \leftarrow S_0$ transition is calculated to be HOMO to LUMO it seems apparent the cyclopentadiene ring is not merely a spectator in the electronic spectrum.

Figure S1: Extended, saturated R2PI showing very weak transitions above 400 cm^{-1} above the electronic origin transition.

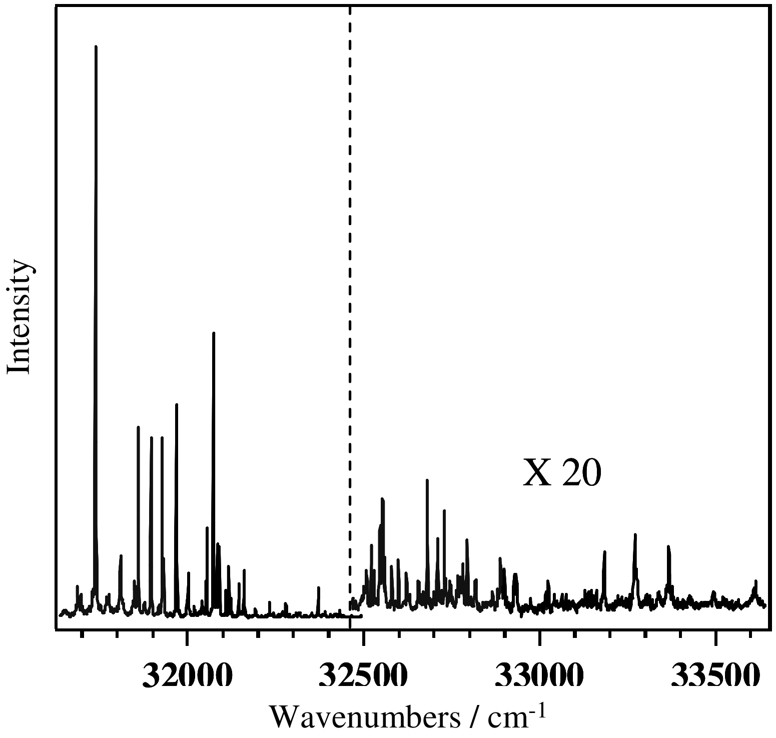

Table S1: Assignments for the LIF spectrum of PCP3D.

Frequency	$\Delta\nu$/cm^{-1}	Assignment	Frequency	$\Delta\nu$/cm^{-1}	Assignment
31688	-51	57^0_2	32018	279	
31696	-43	56^1_1	32040	301	$55^1_0\,57^2_1$
31739	0	0^0_0	32052	313	
31776	37	$56^1_0\,57^0_1$	32055	316	38^2_0
31810	71	57^1_1	32074	335	37^1_0
31849	110	$55^1_0\,57^0_1$	32083	344	
31860	121	56^2_0	32089	350	
31878	139	57^2_2	32107	368	
31897	158	38^1_0	32116	377	57^4_0
31919	180	$55^1_0\,57^2_1$	32121	382	
31927	188	57^2_0	32160	421	
31932	193	$56^2_0\,57^1_1$	32192	453	
31968	229	$55^1_0\,57^1_0$	32232	493	$37^1_0\,38^1_0$
32000	261	57^3_1	32370	631	
32002	263		32553	814	
32014	275				

Table S2: Complete Assignments of the SVLF of PCP3D

Origin	31740 cm^{-1}	37^1_0	0^0_0+334 cm^{-1}	57^2_0	0^0_0+188 cm^{-1}	56^2_0	0^0_0+121 cm^{-1}
Δv / cm^{-1}	Assignment	Δv / cm^{-1}	Assignment	Δv / cm^{-1}	Assignment	Δv / cm^{-1}	Assignment
0	0^0_0	0	37^1_0	0	57^2_0	51	56^2_0 57^0_2
51	57^0_2	50	37^1_0 57^0_2	51	57^2_2	111	56^2_0 57^0_4
112	57^0_4	109	37^1_0 57^0_4	111	57^2_4	127	56^2_1 57^0_1
168	38^0_1	175	37^1_0 57^0_6	126	56^0_1 57^2_1	208	56^2_2
209	56^0_2	208	37^1_0 56^0_2	175	57^2_6	256	56^2_2 57^0_2
349	37^0_1	348	37^1_1	207	56^0_2 57^2_0	349	37^0_1 56^2_0
398	37^0_1 57^0_2	354	37^1_0 56^0_1 57^0_1	245	57^2_8	355	55^0_1 56^2_1
455	37^0_1 57^0_4	478	37^1_0 54^0_1 56^0_1	276	55^0_1 57^2_1	416	56^2_4
503	55^0_2	521	37^1_0 54^0_1 56^0_1 57^0_2	316	57^2_{10}	476	54^0_1 56^2_3
516	37^0_1 38^0_1	577	37^1_0 54^0_1 56^0_1 57^0_4	348	37^0_1 57^2_0	557	37^0_1 56^2_2
558	56^0_2 37^0_1	626	37^1_1 55^0_1 57^0_1	356	55^0_1 56^0_1 55^2_0	603	37^0_1 56^2_2 57^0_2
631	35^0_1	696	37^1_2	397	37^0_1 57^2_2	713	55^0_2 56^2_2
680	34^0_1	703	37^1_1 55^0_1 56^0_1	456	37^0_1 57^2_4	909	37^0_2 56^2_2
697	37^0_2	826	37^1_1 54^0_1 56^0_1	475	37^0_1 56^{01} 57^2_1	1076	32^0_1 56^2_2
743	54^0_2, 37^0_2 57^0_2	865	32^0_1 37^1_0	519	37^0_1 57^2_6		
826	33^0_1	914	32^0_1 37^1_0 57^0_2	557	37^0_1 56^0_2 57^2_0		
866	32^0_1	1046	37^1_3	588	37^0_1 55^0_1 57^2_1		
918	32^0_1 57^0_2	1177	33^0_1 37^1_1	622	37^0_1 55^0_1 57^2_1		
1009	29^0_1	1347	32^0_1 37^1_1 54^0_1 56^0_1	696	37^0_2 57^2_0		
1020	28^0_1			746	37^0_2 57^2_2		
1034	27^0_1			803	37^0_2 57^2_4		
1047	37^0_3			867	37^0_2 57^2_6		
1122	25^0_1			906	37^0_2 56^0_2 57^2_0		
1216	23^0_1						
1265	23^0_1 57^0_2						
1325	23^0_1 57^0_4						
1361	18^0_1						

38^0_1	0^0_0+158 cm^{-1}	57^0_2	0^0_0+188 cm^{-1}	$55^1_0\ 57^1_0$	0^0_0+230 cm^{-1}
Δv / cm^{-1}	Assignment	Δv / cm^{-1}	Assignment	Δv / cm^{-1}	Assignment
0	38^1_0	0	57^2_0	0	$55^1_0 57^1_0$
127	$38^1_0\ 56^0_1\ 57^0_1$	51	57^2_2	51	$55^1_0\ 57^1_2$
166	38^1_1	111	57^2_4	112	55^1_0
211	38^1_1	126	$56^0_1\ 57^2_1$	176	$55^1_0\ 57^1_6$
266	$38^1_1\ 57_{04}$	175	57^2_6	244	$55^1_0\ 57^1_8$
333	38^1_2	207	$56^0_2\ 57^2_0$	276	$55^1_1\ 57^1_1$
374	$38^1_0\ 56^0_2$	245	57^2_8	315	$55^1_0\ 57^1_{10}$
499	38^1_3	276	$55^0_1\ 57^2_1$	335	$38^0_2\ 55^1_0\ 57^1_0$
515	$37^0_1\ 38^1_1$	316	57^2_{10}	349	$37^0_1\ 55^1_0\ 57^1_0$
557	$37^0_1\ 38^1_1\ 57^0_2$	348	$37^0_1\ 57^2_0$	357	$55^1_1\ 56^0_1\ 57^1_0$
613	$37^0_1\ 38^1_1\ 57^0_4$	356	$55^0_1\ 56^0_1\ 55^2_0$	399	$37^0_1\ 55^1_0\ 57^1_2$
671	$38^1_1\ 55^0_2$	397	$37^0_1\ 57^2_2$	456	$37^0_1\ 55^1_0\ 57^1_4$
681	$37^0_1\ 38^1_1$	456	$37^0_1\ 57^2_4$	504	$38^0_3\ 55^1_0\ 57^1_0$
866	$37^0_2\ 38^1_1$	475	$37^0_1\ 56^0_1\ 57^2_1$	520	$37^0_1\ 55^1_0\ 57^1_6$
904	$37^0_2\ 38^1_1 57^1_2$	519	$37^0_1\ 57^2_6$	587	$37^0_1\ 55^1_0\ 57^1_8$
993	$33^0_1\ 38^1_1$	557	$37^0_1\ 56^0_2\ 57^2_0$	625	$37^0_1\ 55^1_1\ 57^1_1$
1033	$32^0_1\ 38^1_1$	588	$37^0_1\ 55^0_1\ 57^2_1$	681	$37^0_1\ 38^0_2\ 55^1_0\ 57^1_0$
1079	$32^0_1\ 38^1_1\ 57^0_2$	622	$37^0_1\ 55^0_1\ 57^2_1$	705	$37^0_1\ 55^1_1\ 56^0_1\ 57^1_0$
1176	$29^0_1\ 38^1_1$	696	$37^0_2\ 57^2_0$	745	$54^0_2\ 55^1_0\ 57^1_0$
1187	$28^0_1\ 38^1_1$	746	$37^0_2\ 57^2_2$	867	$32^0_1\ 55^1_0\ 57^1_0$
1201	$27^0_1\ 38^1_1$	803	$37^0_2\ 57^2_4$	973	$37^0_2\ 55^1_1\ 57^1_1$
1216	$37^0_3\ 38^1_1$	867	$37^0_2\ 57^2_6$	978	$37^0_1\ 55^1_2\ 56^0_1\ 57^1_1$
1289	$25^0_1\ 38^1_1$	906	$37^0_2\ 56^0_2\ 57^2_0$	1028	$37^0_2\ 38^0_2\ 55^1_0\ 57^1_0$
				1055	$37^0_2\ 55^1_1\ 56^0_1\ 57^1_0$
				1203	$32^0_1\ 38^0_2\ 55^1_0\ 57^1_0$
				1216	$32^0_1\ 37^0_1\ 55^1_0\ 57^1_0$
				1223	$32^0_1\ 55^1_1\ 56^0_1\ 57^1_0$

Table S3: Calculated torsional angles and torsional vibrational frequencies for the two isomers of PCPD that are expected to be in the probed spectra region.

		PCP3D		PCP4D	
	Method	Torsional Angle	Torsional Frequency	Torsional Angle	Torsional Frequency
S_0	AM1	0.0	23.4	25.7	46.5
	HF/6-31G	22.1	36.3	36.1	60.9
	HF/6-31+G(d,p)	25.6	38.6	36.5	60.4
	B3LYP/6-31G	0.0	25.7	25.1	55.4
	B3LYP/6-31+G	11.2	26.6	27.1	53.5
	B3LYP/6-31G(d,p)	0.0	20.4	26.5	57.5
	B3LYP/6-31+G(d,p)	12.2	29.3	27.7	54.0
	B3LYP/6-311+G(d,p)	0.0	14.9	28.8	53.7
		15.8	33.3		
	B3LYP/6-311+G(2d,2p)	0.0	17.3	27.0	52.6
	MP2/6-31+G	42.3	53.6	48.2	55.5
S_1	CIS/6-31G	0.0	104.4	9.3	65.6
	CIS/6-31G(d,p)	0.0	102.0	9.8	61.2
	CIS/6-31+G(d,p)	0.0	104.2	3.4	53.5
	CIS/6-311G	0.3	104.8	7.5	64.5
	CIS/6-311+G	0.0	105.4	2.7	57.6
	CIS/6-311+G(d,p)	0.0	105.8	1.8	56.6

Figure S2: Calculated torsional potentials for PCP4D in the S_0 (lower) and S_1 (upper) states. The S_0 potential was calculated at the B3LYP//6-311+G(d,p) level of theory while the S_1 was computed using CIS//6-311+G(d,p).

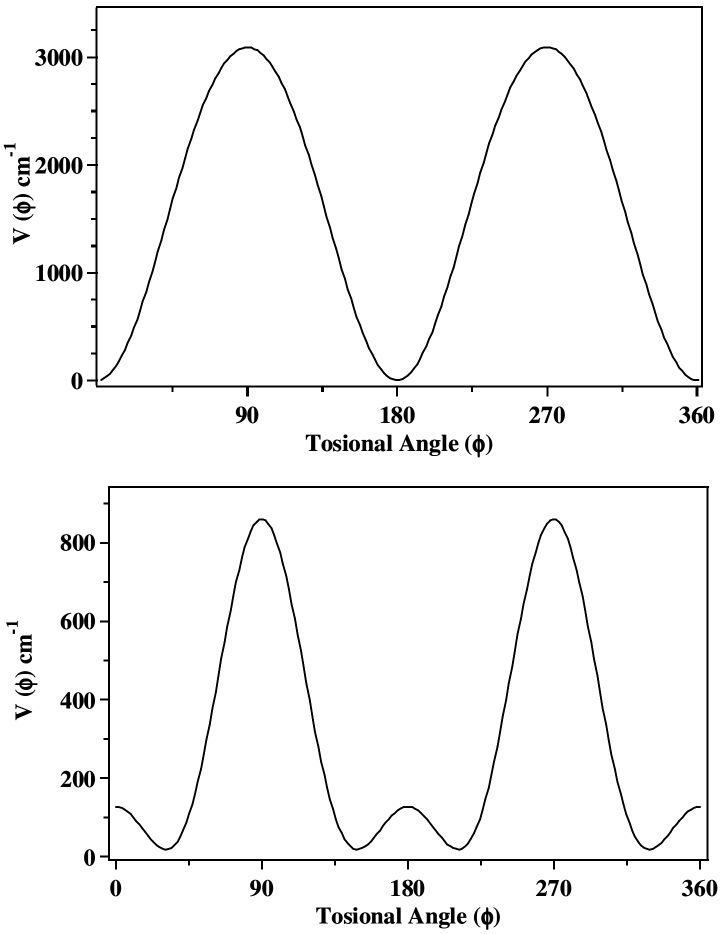

Simulated Franck-Condon Intensities

Absorption intensities, which can be compared to experimental band intensities of R2PI or LIF spectra , were calculated according to

$$\mathrm{I}(\mathrm{T}_0^n) \propto \left(\sum_{i=1}^{N} c_{i0}^{S_0,\mathrm{even}} c_{in}^{S_1,\mathrm{even}} \right)^2 + \left(\sum_{i=1}^{N} c_{i0}^{S_0,\mathrm{odd}} c_{in}^{S_1,\mathrm{odd}} \right)^2 , \qquad (1)$$

whereas emission intensities, which can be compared to the band intensities of SVLF spectra (**Figure 12**), were determined according to

$$\mathrm{I}(\mathrm{T}_n^0) \propto \left(\sum_{i=1}^{N} c_{in}^{S_0,\mathrm{even}} c_{i0}^{S_1,\mathrm{even}} \right)^2 + \left(\sum_{i=1}^{N} c_{in}^{S_0,\mathrm{odd}} c_{i0}^{S_1,\mathrm{odd}} \right)^2 . \qquad (2)$$

For the simulation of the LIF spectrum of PCP3D containing all transitions involving the torsional mode 57, i.e. the origin ($0^0{}_0$), the cold band, $57^2{}_0$, and the hot bands $57^0{}_2$, $57^1{}_1$ and $57^3{}_1$. The knowledge of the Boltzmann factors of the pertinent ground state levels 0_0 57_1 and 57_2 is required. The calculation of the factors is achieved in the following manner.

First, the approximate vibrational temperature T_{vib} is calculated according to

$$\frac{f(57_2^2)}{f(0_0^0)} = \frac{I_{FES}(57_2^2)}{I_{FES}(0_2^2)} \cdot \frac{I_{SVLF_0^0}(0_2^2)}{I_{SVLF\,0_0^0}(57_2^2)} = \exp\left[-\frac{h\nu}{kT_{vib}} \right] \qquad (3)$$

Which yields T_{vib}=9.8K for $\nu(57^0{}_2)$=51 cm^{-1}. This value can be used to calculate the Boltzmann factor for the 57^1 level as

$$\frac{f(57_2^2)}{f(0_0^0)} = 2.8848 \cdot 10^{-2}. \qquad (4)$$

All relative intensities were then simulated according to

$$I(57_m^n)\alpha \left(f_m \sum_{i=1}^{N} c_{cim}^{S0,even} c_{in}^{S1,even} \right)^2 + \left(f_m \sum_{i=1}^{N} c_{cim}^{S0,odd} c_{in}^{S1,odd} \right)^2 \qquad (5)$$

Figure S3: Franck-Condon intensity simulations of the (a) LIF spectrum and (b) SVLF spectrum of the 57^1_1 transitions. The LIF simulation assumes a vibrational temperature of 9.8 K. The resonance fluorescence band was cut off in the 57^1_1 band SVLF spectrum as most of the observed intensity was due to incomplete subtraction of scattered light from the laser.

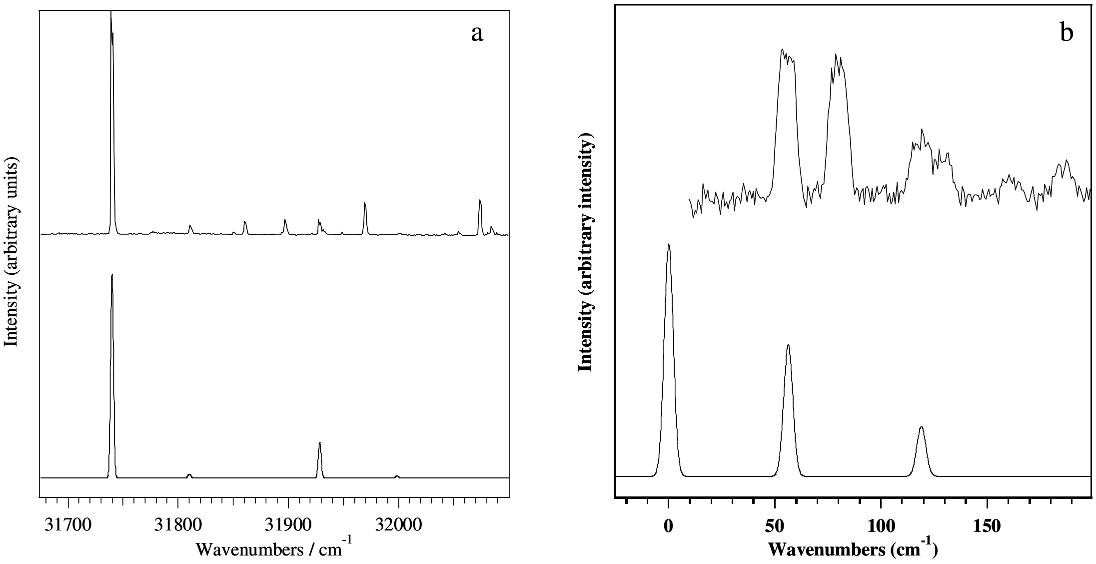

Figure S4: Calculated molecular orbitals (CIS//6-311+G(d,p)) for PCP3D. Since the calculated $S_1 \leftarrow S_0$ transition is calculated to be HOMO to LUMO it seems apparent that the cyclopentadiene ring is not merely a spectator in the electronic spectrum.

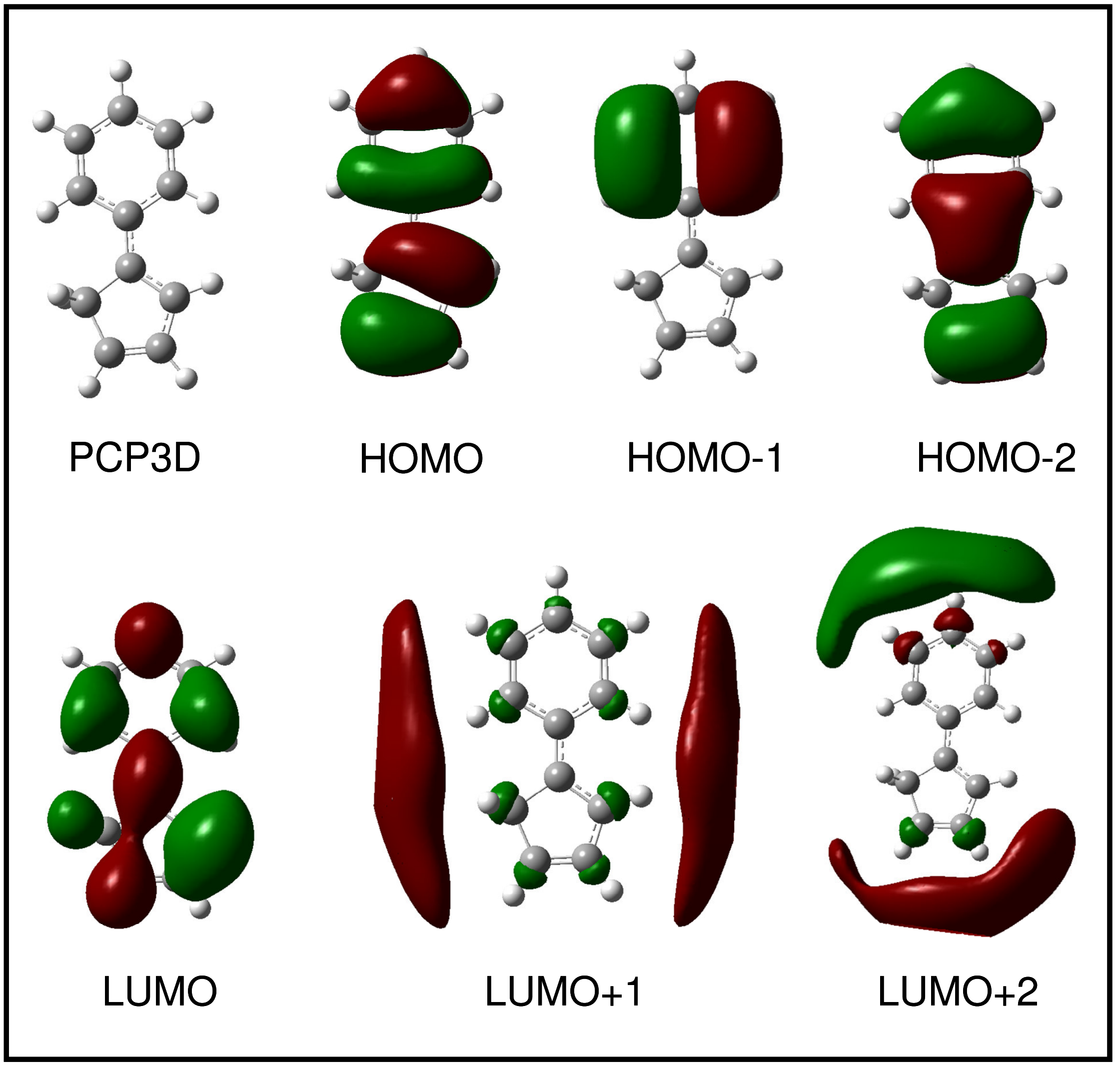

Figure S5: Graphical representation of the vibrational modes of PCP3D

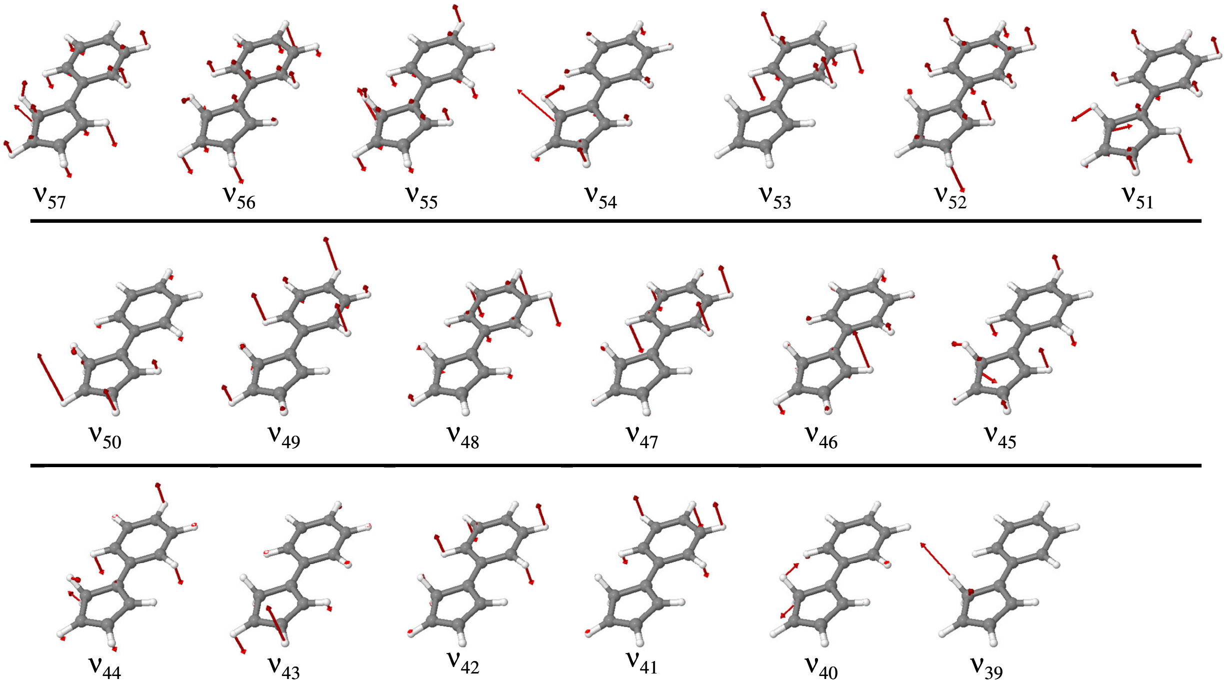

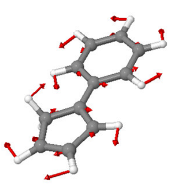
ν_{38}


ν_{37}

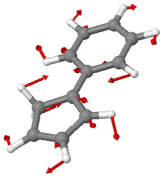
ν_{36}

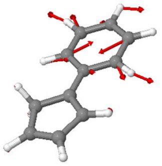
ν_{35}

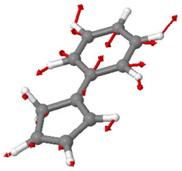
ν_{34}

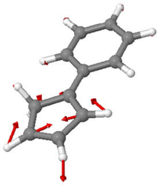
ν_{33}


ν_{32}


ν_{31}

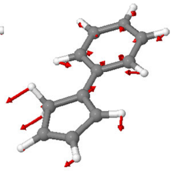
ν_{30}

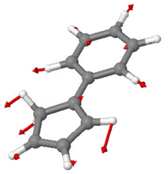
ν_{29}

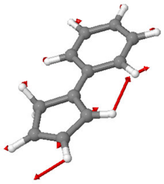
ν_{28}

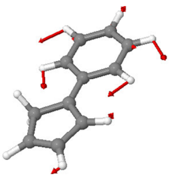
ν_{27}

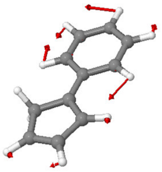
ν_{26}

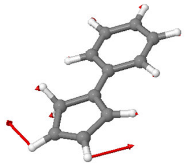
ν_{25}

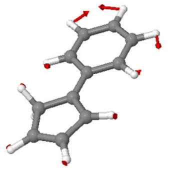
ν_{24}


ν_{23}

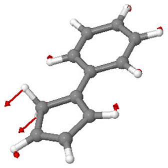
ν_{22}

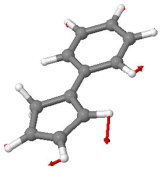
ν_{21}

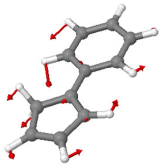
ν_{20}

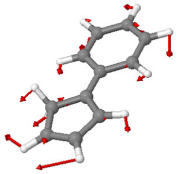
ν_{19}

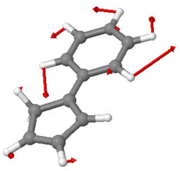
ν_{18}

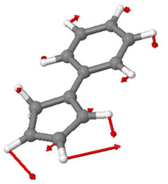
ν_{17}

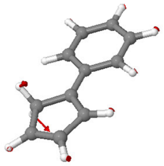
ν_{16}

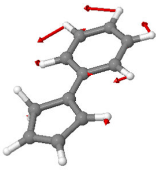
ν_{15}

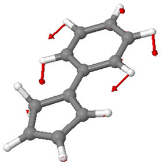
ν_{14}

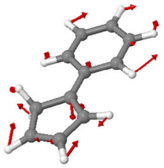
ν_{13}


ν_{12}

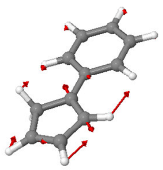
ν_{11}

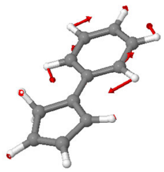
ν_{10}

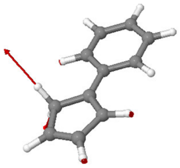
ν_9

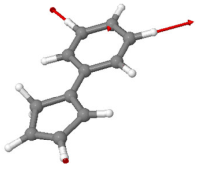
ν_8

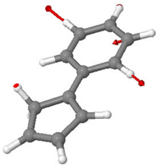
ν_7

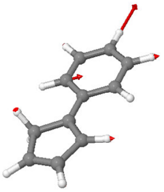
ν_6

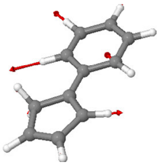
ν_5

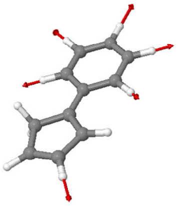
ν_4

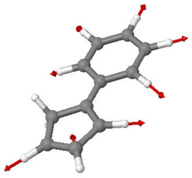
ν_3

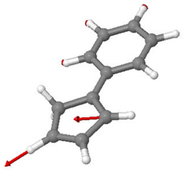
ν_2

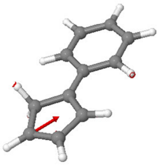
ν_1